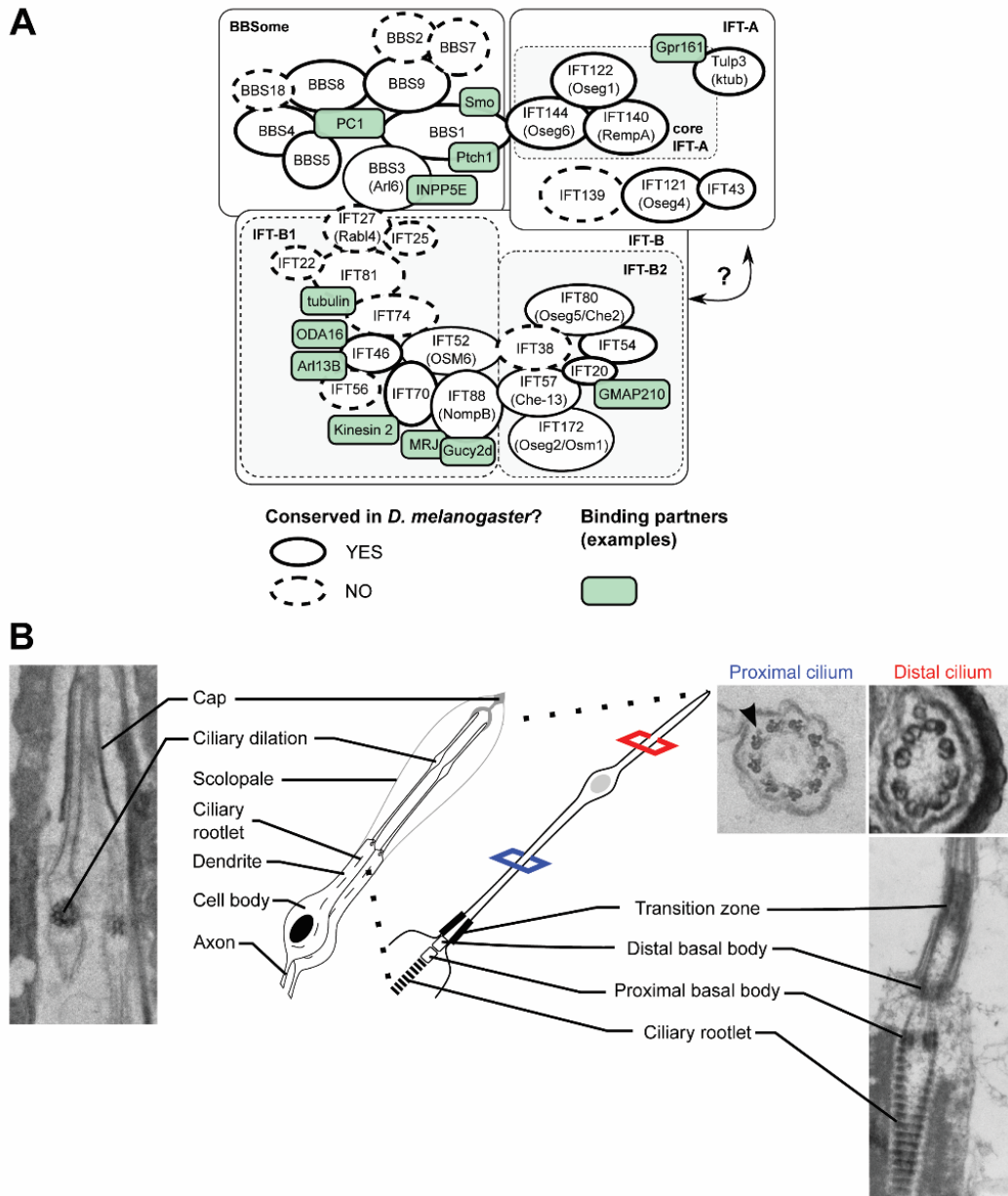


Supplemental Figures and Legends:

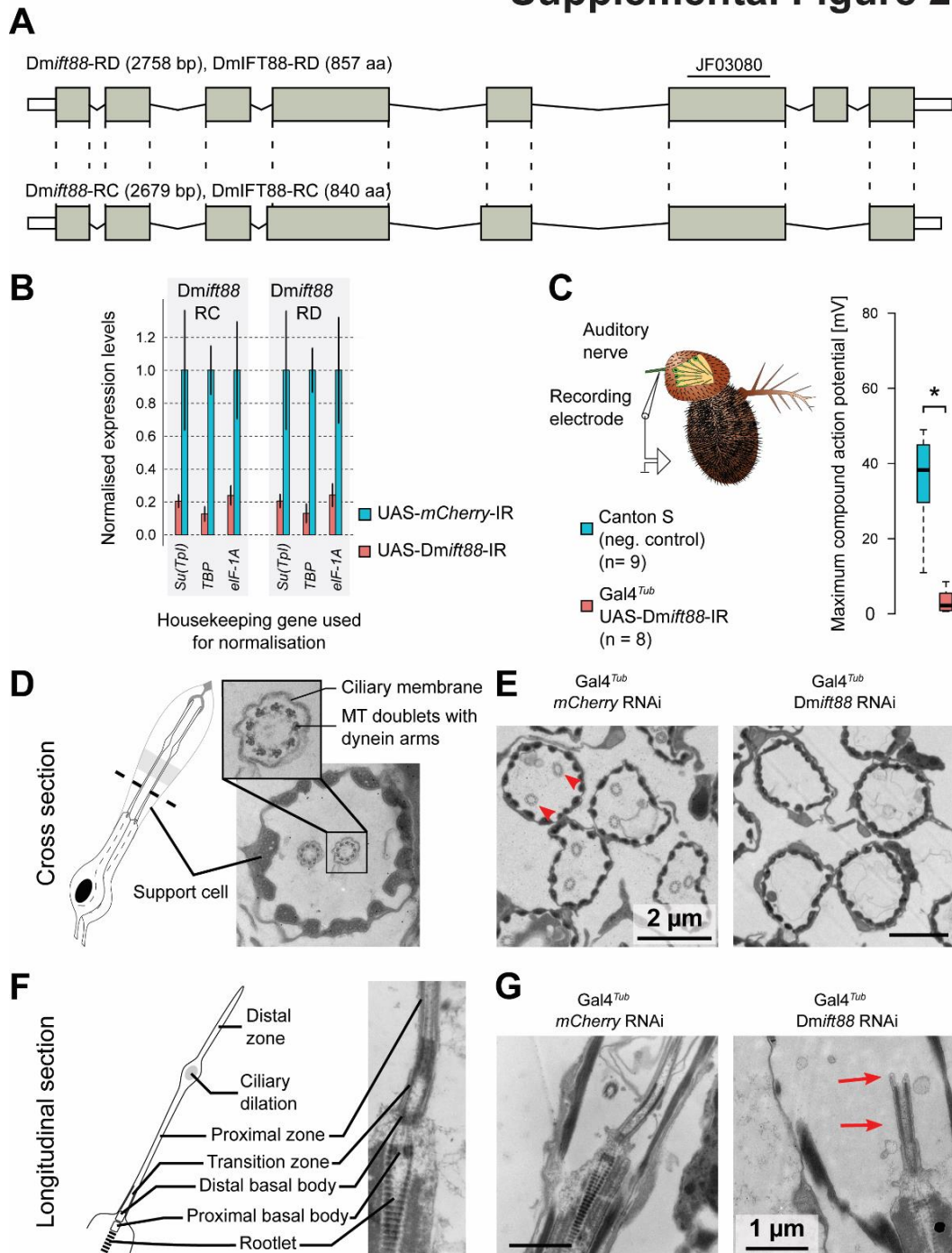
Supplemental Figure 1



Supplemental Figure 1: Conservation of the Intraflagellar Transport (IFT) complex in *Drosophila* and description of the ultrastructure of chordotonal cilia in the adult 2nd antennal segment. (A) Schematic presentation of the components of the IFT complex found in human, *Chlamydomonas* (*C. reinhardtii*) and *Drosophila* (*D. melanogaster*). IFT consists of three complexes: IFT-A, IFT-B and the BBSome. IFT-A and –B are further divided based on their genetic features and biochemical properties. For the IFT-A and –B proteins, the *Chlamydomonas* nomenclature is used. Proteins conserved and not conserved in *Drosophila* are encircled by full and dashed outlines, respectively. The scheme also shows where the three complexes interact

and highlights some known binding partners (green boxes). This scheme is modified from (Mourao et al., 2016). **(B)** Ultrastructural organisation of the cilium of chordotonal neurons in the fly 2nd antennal segment, as seen by electron micrographs. Here, two neurons project their cilia towards a cap cell. Each ciliary shaft is divided by the ciliary dilation into a proximal and a distal zone, which have distinct axonemal architectures, with only the proximal zone harbouring axonemal dynein arms (arrowhead). The base of the cilia is formed by distal and proximal basal bodies and the rootlet (Jana et al., 2016).

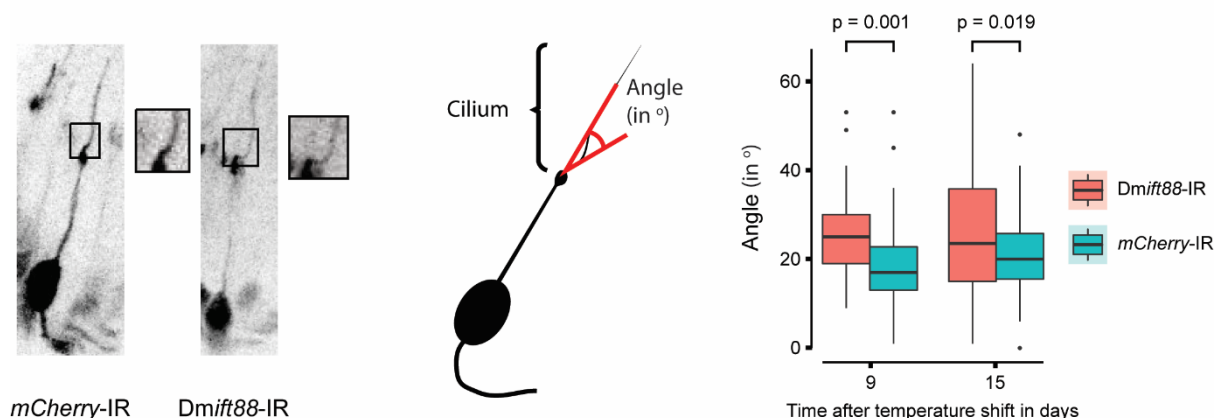
Supplemental Figure 2



Supplemental Figure 2: Validation of the *Dmift88* inverted repeat (IR) used to downregulate *Dmift88* expression. (A) Schematic representation showing that the hairpin (ID: JF03080) affects both *Dmift88* isoforms by targeting a common exon. **(B)** Bar plots (Mean \pm S.D.) of real-time PCR quantification of *Dmift88* isoform levels. mRNA was extracted from the antennae of flies expressing a hairpin against either *mCherry* (negative control) or *Dmift88*. The hairpin expression was driven using the tubulin promoter (*Gal4^{Tub}*). The total mRNA was extracted three times per hairpin and

each RNA sample was measured in triplicates. The data is normalised using three different housekeeping genes (*Su(Tpl)*, *TBP* and *eIF-1A*) to account for potential transcriptional changes of housekeeping genes as a consequence of the knockdown. **(C)** Box plots of maximum sound-evoked compound action potentials of chordotonal neurons in the second antennal segment of wild type flies (Canton S; negative control) and DmIFT88 knockdown flies expressing constitutively *Dmift88*-IR (*Gal4^{Tub}>UAS-Dmift88* RNAi). The sound responses are virtually abolished from the antenna of DmIFT88 knockdown flies (*p-value = $6.274e^{-05}$ from Welch two sample t-test). Action potentials are measured from 4-6 days old flies. Median \pm full range of variation (minimum to maximum). **(D-G)** The flies with knockdown on *Dmift88* using ubiquitously promoter (*Gal4^{Tub}*) do not grow chordotonal cilia. Schematic representation and the representative EM images of wild type chordotonal cilia in cross (D) and longitudinal section (F). Representative images of cross-sections (E) and longitudinal-sections (G) of the chordotonal cilia in the adult flies ubiquitously (*Gal4^{Tub}*) expressing *mCherry*-IR (negative control) or *Dmift88*-IR. Note that upon ubiquitous knockdown of *Dmift88*, chordotonal neurons form ciliary transition zones (red arrows), but fail to extend cilia.

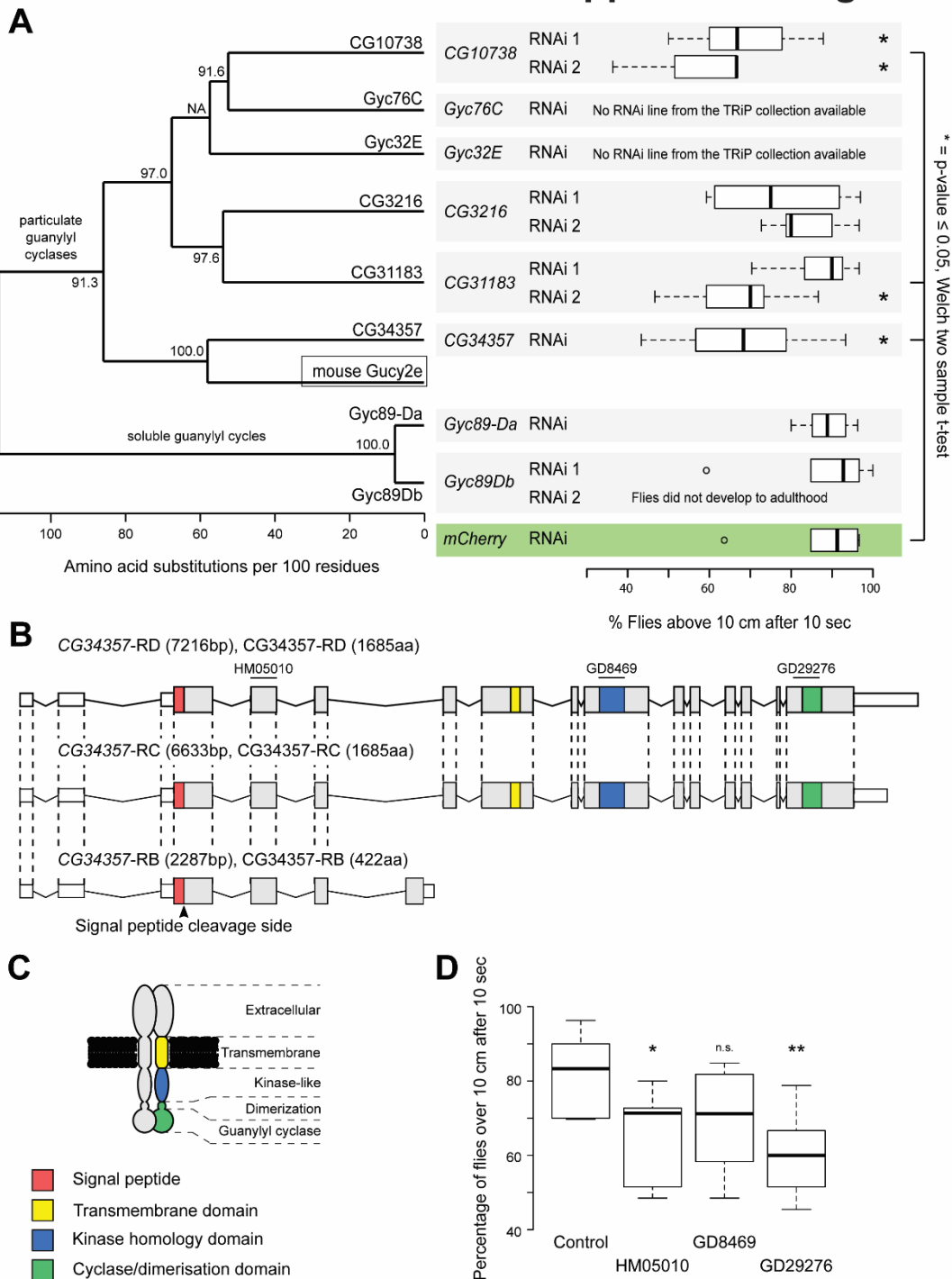
Supplemental Figure 3



Supplemental Figure 3: Continuous knockdown of DmIFT88 in the adult increases the curvature of the axoneme at the base of the cilium. Left: Representative images of chordotonal neurons in the 2nd antennal segment of flies with *mCherry* or *DmIFT88* knockdown for 15 days. Neurons are visualised by co-

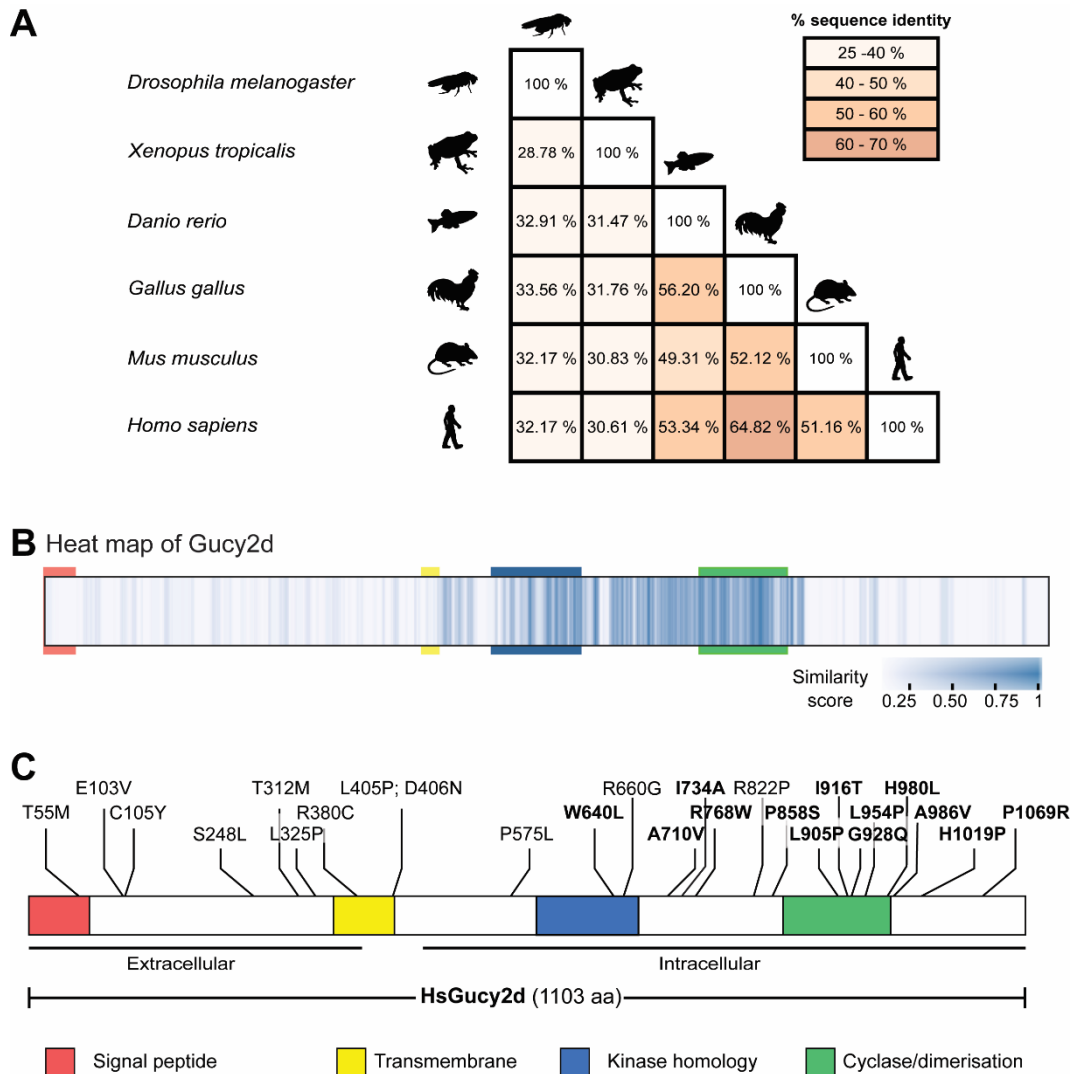
expressing GFP together with the respective hairpin. Long term knockdown of DmIFT88 affects ciliary (axoneme) bending (scheme in the Middle): cilia in DmIFT88 knockdown flies project out at a different angle from the dendrites than cilia in the control flies, as shown in the box plots (right). Data is obtained from antenna whole mounts to avoid artefacts from the sectioning process. Each box plot corresponds to the value of 50 angles from 5 different antennae. p-values are calculated using Welch Two Sample t-test.

Supplemental Figure 4



Supplemental Figure 4: CG34357 is a homologue of mouse Gucy2e and its downregulation in the cholinergic neurons leads to climbing defects. (A) PSI-BLAST search was performed against the fly genome using the mouse Gucy2e protein sequence. All six particulate guanylyl cyclases encoded in the *Drosophila* genome were found in the search (Morton, 2004). The similarity of the protein sequences to each other is shown on the left side (maximum-likelihood phylogenetic tree). Two soluble guanylyl cyclases were included as outgroups. A behavioural screen was

conducted to determine if any of the identified enzymes could be involved in climbing (or gravity sensing), and the results are shown on the right side. The genes were knocked down using RNAi; a hairpin against *mCherry* was used as a negative control. The RNAi was driven using the cholinergic-neuronal driver ($\text{Gal4}^{\text{Chat19b}}$), and flies were raised at 29°C to increase the potential phenotype, as Gal4 is sensitive to temperature. Only fly lines from the TRiP (Transgenic RNAi Project) library were considered (see Methods). When possible, two to three RNAi lines were used against the same gene. Each boxplot corresponds to 60 flies measured in groups of ten flies each. **(B)** *CG34357* gene has three annotated transcripts in the fly. Isoform RC and RD lead to the same protein and only vary in the length of the 3'-UTR. Isoform RB results from one alternative splice event leading to a drastically shorter amino acid sequence containing only extracellular parts of the protein. The different functional domains are colour-coded (legends are described in C). The exons targeted by the hairpins used in D are indicated in the scheme. **(C)** Protein model is drawn analogously to vertebrate particulate guanylyl cyclase (Kuhn, 2016), and functional domains are indicated using the same colours as in B. The signal peptide is not shown in the protein model because it should be cleaved off according to signal peptide prediction (Nielsen, 2017). **(D)** A climbing assay was used to determine the role of *CG34357* in gravity sensing. An RNAi line against *mCherry* was used as a negative control. All RNAis were driven using the $\text{Gal4}^{\text{Chat19b}}$, and the flies were raised at 29°C to increase the potential phenotype. Each boxplot corresponds to a total of 60 flies measured in sets of ten flies each. In A and D, the significance is determined using the Welch two sample t-test (*p-value < 0.05, **p-value < 0.01).



Supplemental Figure 5: Cross species comparison of Gucy2d homologues and overview of known mutations in human Gucy2d in patients with Leber congenital amaurosis (LCA). (A) Matrix shows pair-wise comparison of different Gucy2d homologues between different vertebrate species and *Drosophila melanogaster*. Numbers indicate percentages of identical residues in pair-wise alignments. Even within vertebrate species the sequence identity is rather low. (B) Multiple sequence alignment of Gucy2d from twelve species is represented as a heat map generated using JProfileGrid2 (a list of the species is available in Supplemental Table 3). Each position of the alignment is shown as a box, which is then colour-coded according to the similarity score. The relative positions of the four critical domains of Gucy2d are indicated with the specific-coloured boxes. (C) Known sites mutated in patients with LCA. Residues highlighted in bold are conserved in *Drosophila melanogaster* (Supplemental Table 08). There is no clear hotspot region for mutations in humans (de Castro-Miro *et al.*, 2014; Feng *et al.*, 2020; Jacobson *et al.*, 2013; Li *et*

al., 2011; Liu et al., 2020; Salehi Chaleshtori et al., 2020; Tucker et al., 2004; Zagel and Koch, 2014).

Supplemental Tables:

Supplemental Table 01: IFT and BBSome homologues in various species.

Drosophila homologues were annotated according to <https://flybase.org/>.

	<i>Chlamydomonas reinhardtii</i>	<i>Homo sapiens</i>	<i>Drosophila melanogaster</i>
IFT-A (7 members)	IFT43	IFT43	CG5780
	IFT121	WDR35	Oseg4
	IFT122/FAP	WDR10	Oseg1
	IFT139	THM1/TTC21B	<i>Not conserved</i>
	IFT140	WDTC2	RempA/Oseg3
	IFT144	WDR19	Oseg6
IFT-B (16 members)	IFT20	IFT20	CG30441
	IFT22/FAP9	RabL5	<i>Not conserved</i>
	IFT25/FAP232	IFT25	<i>Not conserved</i>
	IFT27	RabL4	<i>Not conserved</i>
	IFT38/FAP22	Cluap	<i>Not conserved</i>
	IFT46	IFT46	CG15161
	IFT52/Bld1	IFT52	Osm-6
	IFT54/FAP116	TRAF3IP1	CG3259
	IFT56/DYF-13	TTC26	<i>Not conserved</i>
	IFT57	Hippi	Che-13
	IFT70/FAP259	TTC30A/B	<i>Not conserved</i>
	IFT74	IFT74	<i>Not conserved</i>
	IFT80	IFT80	Oseg5
	IFT81	IFT81	<i>Not conserved</i>
IFT88	IFT88	NompB	
IFT172	IFT172	Oseg2	
BBSome (10 members)	BBS1	BBS1	BBS1
	BBS2	BBS2	<i>Not conserved</i>
	BBS3	BBS3	Arl6
	BBS4	BBS4	BBS4
	BBS5	BBS5	BBS5
	BBS6	BBS6	<i>Not conserved</i>
	BBS7	BBS7	<i>Not conserved</i>
	BBS8	BBS8	BBS8
	BBS9	BBS9	BBS9
	BBS18	BBSIP10	<i>Not conserved</i>

Supplemental Table 02: IFT88 protein sequences used for comparison.

Species	Abbreviations	Accession number
<i>Aedes aegypti</i>	Ae	EAT40549
<i>Anopheles gambiae</i>	Ag	XP_556988.3
<i>Danio rerio</i>	Dr	XP_005167586

<i>Drosophila erecta</i>	De	XP_001973983.2
<i>Drosophila melanogaster</i>	Dm	NP_724347.3
<i>Drosophila simulans</i>	Ds	EDX05743.1
<i>Gallus gallus</i>	Gg	XP_015134793.1
<i>Homo sapiens</i>	Hs	NP_001305422
<i>Mus musculus</i>	Mm	NP_033402
<i>Tribolium castaneum</i>	Tc	EFA00677
<i>Xenopus tropicalis</i>	Xt	F6W448

Supplemental Table 03: Protein sequences used for bioinformatic analysis on guanylyl cyclases. Whenever several isoforms were available for the same gene, the longest protein sequence was chosen.

Name	Species	Accession number
Hs_Gucy2d	<i>Homo sapiens</i>	NP_000171
Mm_Gucy2e	<i>Mus musculus</i>	NP_032218
Gg_retGC1	<i>Gallus gallus</i>	AAC24500
Dr_retGC2	<i>Danio rerio</i>	NP_001103165
Xt_retGC1	<i>Xenopus tropicalis</i>	XP_002942678
Ms_GC-II	<i>Manduca sexta</i>	AAN16469.1
Tc_retGC2	<i>Tribolium castaneum</i>	KYB27701.1
Ag_AAEL007359-PA	<i>Aedes aegypti</i>	XP_001658332.1
Ae_AGAP002233-PA	<i>Anopheles gambiae</i>	XP_307952.5
Dm_CG10738	<i>Drosophila melanogaster</i>	NP_729905.2
Dm_CG31183	<i>Drosophila melanogaster</i>	NP_001287342.1
Dm_CG3216	<i>Drosophila melanogaster</i>	NP_726013
Dm_CG34357	<i>Drosophila melanogaster</i>	NP_001189166.1
Dm_Gyc32E	<i>Drosophila melanogaster</i>	NP_001097148.1
Dm_Gyc76C	<i>Drosophila melanogaster</i>	NP_001163473.1
Dm_Gyc89-Da	<i>Drosophila melanogaster</i>	NP_001036718.1
Dm_Gyc89-Db	<i>Drosophila melanogaster</i>	NP_650551.1
De_GG11511	<i>Drosophila erecta</i>	XP_001978835
Ds_GD19673	<i>Drosophila simulans</i>	XP_016033187

Supplemental Table 04: Overview of IFT88 velocities in mouse, *C. elegans* and *Drosophila* (including the results presented in this paper).

Species	Anterograde velocity	Retrograde velocity	Reference
<i>Mus musculus</i> (IMCD3 cells)	0.32 $\mu\text{m/s}$	0.64 $\mu\text{m/s}$	(Besschetnova <i>et al.</i> , 2010)

<i>Mus musculus</i> (IMCD3 cells)	1.19 $\mu\text{m/s}$	1.0 $\mu\text{m/s}$	(Ishikawa <i>et al.</i> , 2014)
<i>Mus musculus</i> (IMCD3 cells)	0.68 $\mu\text{m/s}$	0.35 $\mu\text{m/s}$	(Ye <i>et al.</i> , 2013)
<i>Mus musculus</i> (IMCD3 cells)	0.38 $\mu\text{m/s}$	0.56 $\mu\text{m/s}$	(Tran <i>et al.</i> , 2008)
<i>Mus musculus</i> (MEF)	1.09 $\mu\text{m/s}$	1.06 $\mu\text{m/s}$	(He <i>et al.</i> , 2014)
<i>Mus musculus</i> (olfactory neurons)	0.23 $\mu\text{m/s}$	0.14 $\mu\text{m/s}$	(Williams <i>et al.</i> , 2014)
<i>C. elegans</i>	0.71 $\mu\text{m/s}$ (middle segment); 1.31 $\mu\text{m/s}$ (distal segment)	1.22 $\mu\text{m/s}$	(Wei <i>et al.</i> , 2012)
<i>Drosophila melanogaster</i>	0.44 $\mu\text{m/s}$ (proximal and distal segment)	0.12 $\mu\text{m/s}$ (proximal segment); 0.77 $\mu\text{m/s}$ (outer segment)	(Lee <i>et al.</i> , 2018)
<i>Drosophila melanogaster</i>	0.44 $\mu\text{m/s}$ (proximal segment)	2.09 $\mu\text{m/s}$ (proximal segment)	This study

Supplemental Table 05: Details of the antibodies used in this paper.

Antibody	Dilution	Species	Source
Primary antibodies			
anti-GFP	1:1000	rabbit	Invitrogen, USA
anti-GFP	1:1000	chicken	Aves, USA
anti-GFP	1:1000	rabbit	Roche, Germany
anti-GFP	1:1000	rabbit	Abcam, UK
anti-HA	1:1000	mouse	Biologend, UK
anti-PLP	1:1000	chicken	(Fu and Glover, 2012)
anti-Glutamylated tubulin GT335	1:500	mouse	(Wolff <i>et al.</i> , 1992)
anti-NompC	1:200	rabbit	(Cheng <i>et al.</i> , 2010)
anti-lav	1:500	rat	(Gong <i>et al.</i> , 2004)
anti-acetylated tubulin	1:500	mouse	Sigma, USA
Secondary antibodies			
anti-chicken FITC	1:500	donkey	Jackson Labs, USA

anti-rat Rhodamine	1:500	donkey	Jackson Labs, USA
anti-mouse IRDye 680	1:10000	goat	LI-COR, USA
anti-mouse IRDye 800	1:10000	goat	LI-COR, USA
anti-rabbit IRDye 800	1:10000	goat	LI-COR, USA
anti-rabbit Alexa647	1:10000	donkey	Jackson Labs, USA
anti-rabbit Alexa488	1:500	goat	Molecular Probes, USA
anti-rabbit Alexa647	1:500	donkey	Jackson Labs, USA
anti-chicken Rhodamine	1:500	donkey	Jackson Labs, USA
anti-rat Rhodamine	1:500	goat	Jackson Labs, USA
anti-mouse Alexa488	1:500	goat	Molecular Probes, USA
anti-mouse Alexa647	1:500	goat	Life technologies, USA

Supplemental Table 06: Primers used for the experiments in this paper and the annealing temperatures (T_a) used. The OligoCalc tool was used for prediction (Kibbe, 2007); extension times were chosen according to the length of expected product and the properties of the respective polymerase according to the manufacturer.

Name	Purpose	Sequence	T_a
Dmift88_FL_gateway_fwd	Gateway cloning <i>Dmift88</i>	GGGACAAGTTTGTACA AAAAGCAGGCTTCAT GACTTCTCAAATAACT GCTAACGGAACGC	52°C
Dmift88_FLS_gateway_rev	Gateway cloning <i>Dmift88</i> (with Stop codon)	GGGGACCACTTTGTAC AAGAAAGCTGGGTCTC AAATAGGCAATAAGCT TTCGGG	52°C
Dmift88_seq_fwd	For sequencing <i>Dmift88</i> coding sequence	GCAGCCACAGTGAAACATCG	--
Dmift88_seq_rev	For sequencing <i>Dmift88</i> coding sequence	AACTCAGGTTGGTCAGAGCG	--
Dmift88_seq_rev2	For sequencing <i>Dmift88</i> coding sequence	AGACGGGTGTATTCCGATGC	--
Dmift88-RD_RT-PCR_fwd	Quantify mRNA expression of <i>Dmift88</i> -RD isoform	CCCCTACACGTCCATTCTGC	54°C
Dmift88-RD_RT-PCR_rev	Quantify mRNA expression of	CCCCTACACGTCCATTCTGC	54°C

	Dm <i>ift88</i> -RD isoform		
Dm <i>ift88</i>_RC_RT-PCR_fwd	Quantify mRNA expression of Dm <i>ift88</i> -RC isoform	CGCTGGAATTAGGGGACCTG	54°C
Dm <i>ift88</i>-RC_RT-PCR_rev2	Quantify mRNA expression of Dm <i>ift88</i> -RC isoform	AGGATCAAACCTGCAGAAATC G	54°C
<i>eIF</i>-1A_RT-PCR_fwd	Quantify mRNA expression of <i>eIF</i> 1A (house keeping gene)	GATATACTGGTTCCCCGCGA	54°C
<i>eIF</i>-1A_RT-PCR_rev	Quantify mRNA expression of <i>eIF</i> 1A (house keeping gene)	GGCTTGTGGCGACCAATTTT	54°C
<i>Su(Tpl)</i>_RT-PCR_fwd	Quantify mRNA expression of <i>Su(Tpl)</i> (house keeping gene)	AGCCACAAATCCATGCAGAG	54°C
<i>Su(Tpl)</i>_RT-PCR_rev	Quantify mRNA expression of <i>Su(Tpl)</i> (house keeping gene)	TGGACGTTGACTTCTTGTGT	54°C
TBP_RT-PCR_fwd	Quantify mRNA expression of TBP (house keeping gene)	TTATGCGAATCCGAGAGCCC	54°C
TBP_RT-PCR_rev	Quantify mRNA expression of TBP (house keeping gene)	GTCGAGGAACTTTGCAGGGA	54°C
Dm<i>Gucy2d</i> (CG34356)_5UTR_fwd	Outer primer pair for nested PCR strategy to amplify FL-Dm <i>Gucy2d</i> coding sequence	GGCAATGTTGGAAGGCACTG	52°C
Dm<i>Gucy2d</i>_3UTR_rev	See above	CCCATGTCGTCAGCCATCTA A	
Dm<i>Gucy2d</i>_gateway_FLfw	Gateway cloning of FL Dm <i>Gucy2d</i>	GGGGACAAGTTTGTACAAAA AAGCAGGCTTCATGAAGTTAA CAACCTGTCAAATTGCTAAAG	53°C
Dm<i>Gucy2d</i>_gateway_FLrev	Gateway cloning of FL Dm <i>Gucy2d</i>	GGGGACCACTTTGTACAAGA AAGCTGGGTCTCTGCTCAGC AGTTGCTCTGCATTAAGGG	53°C
Dm<i>Gucy2d</i>_trunc_fwd	Gateway cloning of T1-Dm <i>Gucy2d</i>	GGGGACAAGTTTGTACAAAA AAGCAGGCTTCATGCGTAAG CGTCTCTCCAAGGG	53°C

DmGucy2d_trunc_rev1	Gateway cloning of T2-DmGucy2d	GGGGACCACTTTGTACAAGA AAGCTGGGTCGTTCCGCCGTG GTTGTGATG	53°C
DmGucy2d_trunc_rev2	Gateway cloning of T3-DmGucy2d	GGGGACCACTTTGTACAAGA AAGCTGGGTCTCTGGTTCTT GGCGGAAGTC	53°C
DmGucy2d_trunc_rev3	Gateway cloning of T4-DmGucy2d	GGGGACCACTTTGTACAAGA AAGCTGGGTCAAATTCTTCC GGGTGACGG	53°C
DmGucy2d_trunc_rev4	Gateway cloning of T5-DmGucy2d	GGGGACCACTTTGTACAAGA AAGCTGGGTCAGATTCTCCA ATAGGCGGCG	53°C
DmGucy2d_seq_fwd1	To confirm PCR products through sequencing	TGGCAGGACAATACGTGACC	--
DmGucy2d_seq_fwd2	To confirm PCR products through sequencing	GGACTGGTCGTTTCGGCTAA	--
DmGucy2d_seq_fwd3	To confirm PCR products through sequencing	TCCTGGCGCATCCATATGTC	--
DmGucy2d_seq_rev1	To confirm PCR products through sequencing	GAACCCATGCTGAGTGTCCA	--
DmGucy2d_seq_rev2	To confirm PCR products through sequencing	TTTCTCGAGGTCAAGGCACC	--
DmGucy2d_seq_rev3	To confirm PCR products through sequencing	GGTGGAATTGGAGTCCAGGG	--

Supplemental Table 07: Fly stocks used in this study. (BSC – Bloomington Stock Center, VDRC – Vienna Drosophila Resource Center, DGRC – Drosophila Genomics Resource Center)

Name	Genotype	Source
Gal4^{Tub}	y[1] w[*]; P{w[+mC]=tubP-GAL4}LL7/TM3, Sb[1] Ser[1]	BSC, # 5138
Tub-Gal80^{ts}	w[*]; sna[<i>Sco</i>]/CyO; P{w[+mC]=tubP-GAL80[ts]}7	Made from BSC, #7017
Gal4^{Chat19b}	w[*]; Chat-Gal4/CyO	(Jana et al., 2011)
Gal4^{Chat19b}, UAS-GFP	w[*]; Chat-Gal4, UAS-GFP	(Jana et al., 2011)
Gal4^{lav}	w[*];; lav-Gal4	BSC, # 52273 (a gift from Martin Göpfert's lab)

40xUAS-IVSmCD8::GFP	w[*];; P{y[+t7.7] w[+mC]=40XUAS-IVSmCD8::GFP}attP2	BSC, #32195
UAS-mCD8::GFP	w[*]; UAS-mCD8::GFP/CyO.Z; MKRS/TM6B	a gift from Elio Sucena's lab
UAS-GFP::DmIFT88	W[1];;UAS-GFP::DmIFT88/TM6B	This study (made using IGC Fly transgene facility)
endo-GFP::DmIFT88	w[*]; endo-GFP::DmIFT88	(Han et al., 2003) (a gift from Daniel Eberl)
mCherry RNAi	y[1] sc[*] v[1]; P{y[+t7.7] v[+t1.8]=VALIUM20-mCherry}attP2	BSC, # 35785
Dmift88 RNAi	y[1] v[1]; P{y[+t7.7] v[+t1.8]=TRiP.JF03080}attP2	BSC, # 28665
CG10738 RNAi 1	y[1] v[1];; P{y[+t7.7] v[+t1.8]=TRiP.HMS01814}attP2	BSC, #38346
CG10738 RNAi 2	y[1] v[1];; P{y[+t7.7] v[+t1.8]=TRiP.HM05067}attP2	BSC, #28580
CG31383 RNAi 1	y[1] v[1];; P{y[+t7.7] v[+t1.8]=TRiP.HM05092}attP2/TM3, Sb[1]	BSC, #28604
CG31383 RNAi 2	y[1] v[1]; P{y[+t7.7] v[+t1.8]=TRiP.HMJ22232}attP40	BSC, #58224
CG3216 RNAi 1	y[1] sc[*] v[1];; P{y[+t7.7] v[+t1.8]=TRiP.HM05270}attP2/TM3, Sb[1]	BSC, #31877
CG3216 RNAi 2	y[1] v[1];; P{y[+t7.7] v[+t1.8]=TRiP.HMC04174}attP2	BSC, #55895
DmGucy2d (CG34357) GD29276	w1118;; UAS-IR[GD8469]	VDRC, #29276/GD
DmGucy2d GD8469	w1118; UAS-IR[GD8469]	VDRC, #8469/GD
DmGucy2d HM05010	y[1] v[1];; P{y[+t7.7] v[+t1.8]=TRiP.HM05010}attP2	BSC, #28524
DmGucy2d [NP0270]	y[*] w[*];; P{w[+mW.hs]=GawB}CG34357[NP0270] /TM6, P{w[-]=UAS-lacZ.UW23-1}UW23-1	DGRC, #103574
Gyc89-Da RNAi	y[1] sc[*] v[1];; P{y[+t7.7] v[+t1.8]=TRiP.HM05246}attP2/TM3, Sb[1]	BSC, #30502
Gyc89-Db RNAi 1	y[1] v[1];; P{y[+t7.7] v[+t1.8]=TRiP.HM05207}attP2	BSC, #29529
Gyc89-Db RNAi 2	y[1] v[1]; P{y[+t7.7] v[+t1.8]=TRiP.HMJ22088}attP40	BSC, #58139
UAS-DmGucy2d-T1::GFP	w[*];; UAS- DmGucy2d -T1::GFP/TM6B	This study (made using IGC Fly transgene facility)

UAS-DmGucy2d::GFP	w[*]; UAS-DmGucy2d::GFP/CyO	This study (made using BestGene facility)
UAS-DmGucy2d::GFP	w[*]; UAS-DmGucy2d::GFP/TM3	This study (made using BestGene facility)

Supplemental Table 08: Screenshots of alignments of selected sequences of intracellular domains of Gucy2d from diverse species visualised with “Multiple Alignment Show”. Sequences were aligned using MUSCLE (<http://www.ebi.ac.uk/Tools/msa/muscle/>). In addition to the six species shown in Supplemental Figure 5A, six insects species were included in the analysis to avoid a vertebrate bias in the multiple sequence alignment (Supplemental Table 03). Note that the residues that are mutated in human LCA patients and are evolutionarily conserved are marked with red boxes (de Castro-Miro *et al.*, 2014; Feng *et al.*, 2020; Jacobson *et al.*, 2013; Li *et al.*, 2011; Liu *et al.*, 2020; Salehi Chaleshtori *et al.*, 2020; Tucker *et al.*, 2004; Zagel and Koch, 2014).

W640L

```

Homo sapiens NP_000171.1 GAEGPAALWEGNLA VVSEHC TRGSLQDLLAQR EIKLDWMF 642
CG34357 NP_001189166.1 -----PNRTAMVFDYCSRGSLODVLIMDEIKLDWSF 862
Manduca sexta AAN16469.1 -----NRPALVFDYCGRGSLEDVLTADDIKLDWTF 675
Tribolium castaneum KYB27701.1 -----PPRAALVSEYCARGSLODVLQDDIKLDWSF 593
Drosophila erecta XP_001978835.2 -----PNRTAMVFEFCRGSLODVLIMDEIKLDWSF 839
Drosophila simulans XP_016033187.1 -----PNRTAMVFDYCSRGSLODVLIMDEIKLDWSF 859
Aedes aegypti XP_001658332.1 -----PTRTALVVEHC SRGSLODVLIMDEIKLDWSF 281
Anopheles gambiae XP_307952.5 -----PSRTALVFEHC SRGSLODVLIMDEIKLDWSF 191
Mus musculus NP_001124165.1 -----PGVSA MVLEHCARGSLEDLLQENLRLLDWT 652
Danio rerio NP_001103165.1 -----CGVEAIVTEFCRGSLEDLLVND DVKLDWMF 646
Gallus gallus AAC24500.1 -----CGIFAIVSEHC SRGSLEDLLRNQDMKLDWMF 606
Xenopus tropicalis XP_002942678.2 -----PTRILLVTDYCAKGSLYDIENEDIKLDL 650

```

A710V

```

Homo sapiens NP_000171.1 ITD HGHGRLEA QKVL P--EPPRAEDQLWTAPELLRDPAL 719
CG34357 NP_001189166.1 ITD YGLNSFYESQGLPP--RTRSAKELLWTAPELLRNMKL 940
Manduca sexta AAN16469.1 VSDYGLPAFYRAQALPQ--PERSARELLWTAPELLRERRG 753
Tribolium castaneum KYB27701.1 VTDYGLPAFYEAQGMQP--PAKTARELLWTAPELLRHASL 671
Drosophila erecta XP_001978835.2 ITD YGLNSFYESQGLPP--RPRSAKELLWTAPELLRNMKH 917
Drosophila simulans XP_016033187.1 ITD YGLNSFYESQGLPP--RPRSAKELLWTAPELLRNMKL 937
Aedes aegypti XP_001658332.1 ITD YGMLNFD A QGITP--PSKSAKDLLWTAPEALRATKG 359
Anopheles gambiae XP_307952.5 ITD YGMLSFYEAQGIAP--APRNAKELLWTAPEALRDSRT 269
Mus musculus NP_001124165.1 ITD HGYAEFLES HCSSR--PQPAPPELLWTAPELLRGP-- 727
Danio rerio NP_001103165.1 ITD YGYNEVLESQRFPY--IEPPAEDLLWTAPEILRGSYP 723
Gallus gallus AAC24500.1 VTD HGYNELLEAQRVPT--PTPQPQERLWTAPELLRDAAL 683
Xenopus tropicalis XP_002942678.2 VTD FGLHELRLQCAENESIGEHQHYRNQLWRAPPELLRNH-- 728

```

I734A

```

Homo sapiens NP_000171.1 E-----RRGTLAGDVFSLAIIIMQEVVCRSAPY 746
CG34357 NP_001189166.1 HQ----HHHQHGRIQLGTQLGDVYSFGIIMQEVVVRGEPY 976
Manduca sexta AAN16469.1 GG-----GWGATQPGDVFSFAIIMQEVIVRGEFY 782
Tribolium castaneum KYB27701.1 R-----KKGTQPGDVYSFGIIVLQEVVVRGEPY 698
Drosophila erecta XP_001978835.2 HQHQHHHQHGRIQLGTQLGDVYSFGIIMQEVVVRGEPY 957
Drosophila simulans XP_016033187.1 HQHQHHHHHQHGRIQLGTQLGDVYSFGIIMQEVVVRGEPY 977
Aedes aegypti XP_001658332.1 YP-----KGGTQAADVYAFGIIMQEVVVRGEPF 387
Anopheles gambiae XP_307952.5 YP-----KAGTQPADVYAFGIIMQEVVVRGEPY 297
Mus musculus NP_001124165.1 -----GKATFKGDVFSLAIIIIQEVLTTRDPPY 753
Danio rerio NP_001103165.1 G-----LHGTHSGDVYSFSIIMQEVVMRGPFF 750
Gallus gallus AAC24500.1 E-----RRGSFRGDVYGTIGIIMQEVICRSAPY 710
Xenopus tropicalis XP_002942678.2 -----IHGSQKGDVYAFAIIMYEIIFSRKGF 754
    
```

R768W

```

Homo sapiens NP_000171.1 AMLELTPEEVVQRVRSPP-----PLCRPLVSMDAQPV 778
CG34357 NP_001189166.1 CMLSLSPEEIIIVKIKKPP-----PLIRPSVSKGAAPP 1008
Manduca sexta AAN16469.1 CMLALTPDEIVEKVSRRPP-----PLIRPSVSMGAAPP 814
Tribolium castaneum KYB27701.1 CMLALTPPEEIIIEKVKRPP-----PLIRPSVSKGAAPP 730
Drosophila erecta XP_001978835.2 CMLSLSPEEIIIVKIKKPP-----PLIRPSVSKGAAPP 989
Drosophila simulans XP_016033187.1 CMLSLSPEEIIIVKIKKPP-----PLIRPSVSKGAAPP 1005
Aedes aegypti XP_001658332.1 CMLSLSPEEIIIAKIKKPP-----PLIRPSVSKGAAPP 419
Anopheles gambiae XP_307952.5 CMLSLSPEEIIIAKIKKPP-----PLIRPSVSKGAAPP 329
Mus musculus NP_001124165.1 CSWGLSAEEIIRKVASPP-----PLCRPLVSPDQGPL 785
Danio rerio NP_001103165.1 CMLENTEDEIVQKVRKPP-----PMCRPIVSPDHAPM 782
Gallus gallus AAC24500.1 CMLGLPPEEIIIEKVARPP-----PLCRPAVSADQAPL 742
Xenopus tropicalis XP_002942678.2 GQINFEPKEIVDYVKKLPLKGEDPFRPEVESIIEAESCPD 794
    
```

P858S

```

Homo sapiens NP_000171.1 SMLRMLEQYSSNLEDLIRERTEELELEKQKTDRLLTQMLP 858
CG34357 NP_001189166.1 TMFQMLEKYSNNLEELIRERTEQLDIERKKTEQLLNRMLP 1088
Manduca sexta AAN16469.1 SMFEMLEKYSNNLEELIKERTEQLDMEKKKTEQLLNRMLP 894
Tribolium castaneum KYB27701.1 TMFQMLEKYSNNLEELIRERTEQLDIEKKKTEQLLNRMLP 810
Drosophila erecta XP_001978835.2 TMFQMLEKYSNNLEELIRERTEQLDIERKKTEQLLNRMLP 1069
Drosophila simulans XP_016033187.1 TMFQMLEKYSNNLEELIRERTEQLDIERKKTEQLLNRMLP 1089
Aedes aegypti XP_001658332.1 TMFQMLEKYSNNLEELIRERTEQLDMERKKTEQLLNRMLP 499
Anopheles gambiae XP_307952.5 TMFQMLEKYSNNLEELIRERTEQLDIERKKTEQLLNRMLP 409
Mus musculus NP_001124165.1 SMLRMLEKYSSELEDLVQERTEELELERKTERLLSQMLP 865
Danio rerio NP_001103165.1 SMLRMLEQYSSNLEELIRERTEELEIEKQKTEKLLTQMLP 862
Gallus gallus AAC24500.1 SMLRMLEQYSSNLEDLIRERTEELEIEKQKTDKLLTQMLP 822
Xenopus tropicalis XP_002942678.2 QMEMMEKYANNLEDIVTERTRLLCCEKMKTEDLLHRMLP 874
    
```

L905P, I916T, G928Q

```

Homo sapiens NP_000171.1 IEVVDLLNDLYTLFDATIGSHDVYKVETIGDAYMVASGLP 938
CG34357 NP_001189166.1 VQVVDLLNDLYTLFDATINAYNVYKVETIGDAYMVVSGLP 1168
Manduca sexta AAN16469.1 VQVVDLLNDLYTLFDAAIEQYRVYKVETIGDAYMVVGGLP 974
Tribolium castaneum KYB27701.1 EQVVDLLNDLYTTCFDATINAYNVYKVETIGDAYMVVGGLP 890
Drosophila erecta XP_001978835.2 VQVVDLLNDLYTLFDATINAYNVYKVETIGDAYMVVSGLP 1149
Drosophila simulans XP_016033187.1 VQVVDLLNDLYTLFDATINAYNVYKVETIGDAYMVVSGLP 1169
Aedes aegypti XP_001658332.1 VQVVDLLNDLYTTCFDATINAYNVYKVETIGDAYMVVGGLP 579
Anopheles gambiae XP_307952.5 VQVVDLLNDLYTTCFDATINAYNVYKVETIGDAYMVVSGLP 489
Mus musculus NP_001124165.1 IEVVGFLLNDLYTLFDAVLDSDHDVYKVETIGDAYMVASGLP 945
Danio rerio NP_001103165.1 IEVVDLLNDLYTTFDAVIGNHDVYKVETIGDAYMVASGVV 942
Gallus gallus AAC24500.1 IEVVDLLNDLYTLFDVIGCAHDVYKVETIGDAYMVASGLP 902
Xenopus tropicalis XP_002942678.2 LQVVNELLNDLYTVFDRIIRGYDVYKVETIGDAYMVVSGLP 954
    
```

L954P

```

Homo sapiens NP_000171.1 QRNGQRHAAEIANMSLDILSAVGTFRMRHMPEVPPVIRIRIG 978
CG34357 NP_001189166.1 VKIPD-HAEQIATMALDLLHQSGRFNVKHLPGVPLQLRIG 1207
Manduca sexta AAN16469.1 KRARD-HAESVATMALHLLHLAGRFRVRHLPDTPHLRIG 1013
Tribolium castaneum KYB27701.1 VRVPD-HAEQIATMALDLLHQSGRFRIHLPGLTPLRIRIG 929
Drosophila erecta XP_001978835.2 VKIPD-HAEQIATMALDLLHQSGRFNVKHLPGVPLQLRIG 1188
Drosophila simulans XP_016033187.1 VKIPD-HAEQIATMALDLLHQSGRFNVKHLPGVPLQLRIG 1208
Aedes aegypti XP_001658332.1 VRTPD-HAEQIATMALDLLHQSGNFKVRHLPGLVPLQLRIG 618
Anopheles gambiae XP_307952.5 VRTPD-HAEQIATMALDLLSQSGHFKVRHLPGLVPLQLRIG 528
Mus musculus NP_001124165.1 RRNGNRHAAEIANLALDILSYAGNFRMRHAPDVPVIRVRAG 985
Danio rerio NP_001103165.1 VPNGNRHAAEIANMALDILSAVGTFRMRHMPEVPPVIRIRIG 982
Gallus gallus AAC24500.1 KRNGNRHAGEIANMSLDILSSVGTFKMRHMPEVPPVIRIRIG 942
Xenopus tropicalis XP_002942678.2 IKNQDRHAGEIASMALELLHAVKQHRIAHRPNETLKLIRIG 994
    
```

H980L, A986Vfs*76

```

Homo sapiens NP_000171.1 LHS1GPCVAGVVGLTMPRYCLFGDVTNTASRMESTGLPYRI 1018
CG34357 NP_001189166.1 LHTGPCAGVVGLTMPRYCLFGDVTNTASRMESTGSSWRI 1247
Manduca sexta AAN16469.1 LHS1GPCAGVVGLTMPRYCLFGDVTNTASRMESTGAAWRI 1053
Tribolium castaneum KYB27701.1 LHTGPCAGVVGLTMPRYCLFGDVTNTASRMESTGAAWRI 969
Drosophila erecta XP_001978835.2 LHTGPCAGVVGLTMPRYCLFGDVTNTASRMESTGSSWRI 1228
Drosophila simulans XP_016033187.1 LHTGPCAGVVGLTMPRYCLFGDVTNTASRMESTGSSWRI 1248
Aedes aegypti XP_001658332.1 LHTGPCAGVVGLTMPRYCLFGDVTNTASRMESTGSSWRI 658
Anopheles gambiae XP_307952.5 LHTGPCAGVVGLTMPRYCLFGDVTNTASRMESTGSSWRI 568
Mus musculus NP_001124165.1 LHS1GPCVAGVVGLTMPRYCLFGDVTNTASRMESTGLPYRI 1025
Danio rerio NP_001103165.1 LHTGPCVAGVVGLTMPRYCLFGDVTNTASRMESTGLPYRI 1022
Gallus gallus AAC24500.1 LHS1GPCVAGVVGLTMPRYCLFGDVTNTASRMESTGLPYRI 982
Xenopus tropicalis XP_002942678.2 MHTGPV2VAGVVGLTMPRYCLFGDVTNTASRMESNGEALKI 1034
    
```

H1019P

```

Homo sapiens NP_000171.1 HVNLS1TVGILRALDSGYQVELRGRTELKKGAE2DFWLVG 1058
CG34357 NP_001189166.1 HMSQETRDRLDA-RGGYAI1EP2RGLIDIKGKGMNTEFWLLG 1286
Manduca sexta AAN16469.1 QTSAAATAEKL1LA-AGGYRLRSRGLTQIKGK2GAMHTYWLLG 1092
Tribolium castaneum KYB27701.1 HISEATKERLEK-AGGYQLE1YRGPT2EIKGKGMHTYWLLG 1008
Drosophila erecta XP_001978835.2 HMSQETRDRLDA-RGGYDIEQRGLIDIKGKGMNTEFWLLG 1267
Drosophila simulans XP_016033187.1 HMSQETRDRLDA-RGGYAI1EP2RGLIDIKGKGMNTEFWLLG 1287
Aedes aegypti XP_001658332.1 HMSQQT1CN2LLEQ-AGGYIIEPRGPIEIKGKGMHTYWLLG 697
Anopheles gambiae XP_307952.5 HMSQQT1CN2LLEK-AGGYVIEPRGPIEIKGKGMHTYWLLG 607
Mus musculus NP_001124165.1 HVSQSTVQALLSLDEGYKIDV1RGQTE2LKKGLEETYWLTG 1065
Danio rerio NP_001103165.1 HVHSSTVKILMELKLG1YRVELR2ARTE3LKGRIEETYWLTG 1062
Gallus gallus AAC24500.1 HVNARTVAILRALQEGFKLDI1RKTE2LKKGVEDTYWLVG 1022
Xenopus tropicalis XP_002942678.2 HHSNKCKLALDKLGGYITE1KRGLVNMK2KG3DVV4TWVLTG 1074
    
```

P1069R

```

Homo sapiens NP_000171.1 -----RRGFNKPIPK1PPDL----- 1072
CG34357 NP_001189166.1 -----KKGFDKPLPAPPPI1GESHGLDESLIRNSITLKAQ 1320
Manduca sexta AAN16469.1 -----KEG1DRPLPT2PPPL-----ESEEEILVEA----- 1116
Tribolium castaneum KYB27701.1 -----KAGFDKPLP1PPSL-----ELDESLIISK----- 1032
Drosophila erecta XP_001978835.2 -----KKGFDKPLPAPPPI1GESHGLDESLIRNSITLKAQ 1301
Drosophila simulans XP_016033187.1 -----KKGFDKPLPAPPPI1GESHGLDESLIRNSITLKAQ 1321
Aedes aegypti XP_001658332.1 -----KKGFDK1VLP2PPPI3----GLDIAILRKS4L5FQSEQ 727
Anopheles gambiae XP_307952.5 -----KKGFDKALP1PPPI2----GLDVAILKHS3L4FQSQQ 637
Mus musculus NP_001124165.1 -----KVGFCR1PLPT2PLSI----- 1079
Danio rerio NP_001103165.1 -----RDGFTK1PLP2PPVL----- 1076
Gallus gallus AAC24500.1 -----REGFTK1PIPT2PPDL----- 1036
Xenopus tropicalis XP_002942678.2 ANENAIQKKLVDMMDM1PPPL-----FSRPRKSPKLNPD 1107
    
```

Materials and methods:

Bioinformatics analysis

For IFT88: The gene model for *Dmift88* was extracted from the Ensembl Genome Browser (Yates et al., 2016). The number of tetratricopeptide repeat domains (TPR) was predicted using the TPRpred tool (Karpenahalli et al., 2007). For phylogenetic analysis, IFT88 protein sequences of eleven metazoan species were used (see Supplemental Table 02). Whenever several *ift88* isoforms were reported for one species, the largest one was chosen for analysis. The MegAlign program (Lasergene suite, Version 8.1.3, DNASTAR©) was used to generate a phylogenetic tree summarising sequence similarities as a function of the number of amino acid substitutions between sequences. Sequences were aligned using the ClustalW algorithm with default settings. Bootstrapping analysis was performed with default values to calculate the “support value” of each branching point in the tree (Figure 1Aii left). Multiple sequence alignments are presented as a heatmap. An alignment file in the FASTA format using the web browser-based MUSCLE tool was created (Edgar, 2004) to extract sequence identities. Subsequently, the ProfilGrid tool (Roca et al., 2008) was used with default settings to assign a similarity score to each position in the alignment, with the score assuming values between 0 and 1. The results are presented as a heatmap, which was visualised with RStudio (RStudio®, USA) and the ggplot2 package (Wickham, H. (2016). ggplot2. Use R! doi:10.1007/978-3-319-24277-4) (Figure 1Aii right).

For guanylyl cyclases, including *DmGucy2d/CG34357*: Sequence analysis for guanylyl cyclases (Supplemental Figure 3A) was performed as described above. For the accession number of guanylyl cyclases protein sequences used in this analysis, see Supplemental Table 03. The gene model for *CG34357* was taken from the Ensembl Genome Browser (Yates et al., 2016).

Cryosectioning, immunolabeling and image analysis

Histological sections of the adult antenna were prepared as described before (Jana et al, 2016, Mishra, 2015). If not stated otherwise, preparation steps were carried out at room temperature. Flies were anaesthetised using CO₂ and decapitated. The heads were collected in pre-cooled fixation buffer (4% paraformaldehyde, 75 mM PIPES buffer (pH 7.6), 0.05% Triton-X, picric acid) and incubated for 40 minutes. Good

fixation requires the heads to sink to the bottom of the reaction tube. The heads were washed three times in PBST (PBS with 0.05% Triton-X) and then incubated on a rotator in PBST with 10% sucrose, first for one hour at room temperature and then, overnight, in 25% at 4°C. The heads were embedded and oriented appropriately in OCT (optimal cutting temperature formulation; Tissue-Tek, Sakura Finetek, USA) and the OCT was frozen on dry ice. Head samples were sectioned at 12 µm thickness in a Leica Cryostat CM 3050 S (Leica, Germany). The slices were collected on Polyllysine coated slides (Sigma, USA).

Sections were washed with PBST (PBS with 0.05% Triton-X) three times for 10 minutes each, followed by incubation in blocking buffer (10% BSA in PBST) for one hour and subsequent incubation with the primary antibody diluted in blocking buffer overnight at 4°C. Samples were washed three times in blocking buffer and incubated for one hour with secondary antibody in blocking buffer. Finally, after three additional washing steps using PBS for 5 minutes each, samples were embedded in Vectashield supplemented with DAPI (Vector Laboratories). 12-bit images were acquired on a TCS SP5 upright confocal microscope (Leica, Germany) using an PL APO CS 63.0x1.40 OIL objective with a pinhole at 1 Airy unit and a pixel size of 80-200 nm (lateral) and 400nm (axial). For details of the antibodies used, see Supplemental Table 05.

To quantify in the DmIFT88 knockdown experiments the signal intensities of Inactive (lav; a marker for the proximal cilium) antibody staining, and the GFP signal of the T1-DmGucy2d::GFP at the proximal cilium (Figures 2D, 9 days old flies; and Figure 5E, 6 days old flies), image stacks were analyzed with the Imaris software v.9.2.1 (Bitplane). For Figure 2D: The lav channel was used to generate segmented volume surfaces and the lav intensity values were retrieved from Imaris, averaged per antennae in Excel (Microsoft Office, USA) and normalised to the negative control of each repeated experiment. For Figure 5D: The lav channel was used to generate segmented volume surfaces. Next, mean intensity values of lav antibody staining, and T1-DmGucy2d::GFP at the segmented lav surfaces, were retrieved from Imaris, averaged per antennae in Excel (Microsoft Office, USA), and statistically analysed (non-parametric Mann-Witney t-test or Welch Two Sample t-test) in Prism (GraphPad Software, USA). Data were represented on box plots (median ± full range, each dot representing individual averaged values) using Prism 5.2.

To quantify the T1-DmGucy2d::GFP intensity at the end of the dendrites in the adult chordotonal neurons (Figure 5F), the image stacks were deconvolved using the Huygens Deconvolution v17.4 software (Scientific Volume Imaging) with an CMLE algorithm followed by image analysis in Imaris (as mentioned above). This deconvolution step facilitated the segmentation of the crowded dendrite population in the adult antennae by increasing the signal-to-noise ratio (SNR). N>10 antenna in all conditions.

mRNA isolation from adult antenna and reverse transcription analysis

Between 100 and 200 flies were decapitated per genotype. Heads were collected in Protein LoBind tubes (Eppendorf, USA) on dry ice. 10 to 20 heads were collected at a time to avoid compromising of the tissue due to long exposure to room temperature. Tubes were snap-frozen in liquid nitrogen. Antennae were dissociated from heads through mechanical force using a vortex mixer (three times for ten seconds, cooled in between again on dry ice). To separate antennae from heads, tubes were opened and inverted. Heads will fall out, whereas the majority of the antennae will adhere to the wall of the tubes. Total mRNA was isolated from antennae using the PureLink™ RNA Mini Kit (Ambion life technologies, USA). Antennae were lysed in 250 µl of lysis buffer. The protocol was carried out as described in the accompanying manual of the kit. No DNase treatment was performed. The mRNA was always converted to cDNA immediately. For cloning, 1 µg of total mRNA was reverse transcribed. The reverse transcription reaction was performed with the Transcriptor First Strand cDNA Synthesis kit (Roche, Germany). For quantifying mRNA levels, 50 to 70 heads were used. For cloning *Dmift88*, cDNA was generated using poly-dT primers included in the kit. The cDNA samples were stored at -20°C until further use.

Cloning and generation of transgenic flies

For DmIFT88: The cDNA for cloning *Dmift88* was obtained from mRNA isolated from antennae of *w¹¹¹⁸* flies. *Dmift88* (isoform-RD) was amplified using the KOD polymerase kit (EMD Millipore, USA) in 50 µl reaction volume (for PCR primers see Supplemental Table 06). PCR was set up as outlined for the kit. The reaction mix was supplemented with DMSO. The PCR product was purified using the DNA Clean & Concentrator™ kit (Zymo Research, USA) and adenylated at the 5' ends through incubation with DreamTaq (Thermofisher, USA) using the appropriate buffer and

dNTPs at 70°C for one hour. Subsequently, the PCR product was ligated into pGEM-Teasy (Promega, USA) following the manufacturer's instructions and plasmids were confirmed through sequencing (for sequencing primers see Supplemental Table 06). Using the Gateway system, the coding sequence was first cloned into pDONR 221 in a BP-reaction (Invitrogen), following the instructions for the kit, and subsequently transferred to pTHW and pTGW in an LR-reaction (Invitrogen, USA) to fuse the resulting protein to three HA-tags or one GFP-tag on the N-terminus, respectively (for details on pTHW and pTGW see Drosophila Genomic Resource Center, USA). DmIFT88 was tagged at the N-terminus, because the GFP::DmIFT88 fusion protein was previously shown to rescue the *ift88/nompB* mutant phenotype and can hence be considered fully functional (Han et al., 2003).

For DmGucy2d/CG34357 full length (FL) and truncated T1-DmGucy2d GFP constructs: The CG34357 coding sequence was cloned from mRNA isolated from antennae of *w¹¹¹⁸* flies as described above. DmGucy2d could only be amplified from cDNA produced with random hexamer primers (included in the Transcriptor First Strand cDNA Synthesis kit, Roche, Germany). For primer sequences, see Supplemental Table 06. To enhance the chance to amplify the desired target (coding sequence of CG34357-RD, Supplemental Figure 4B) even further, the mRNA was reverse-transcribed using a primer on the 3'-untranslated region of DmGucy2d (CG34357_3UTR_rev 2 µM in a 20 µl reaction volume, 1 µg of total mRNA were used as template). Two rounds of PCRs were performed to obtain the DmGucy2d with the appropriate overhangs for Gateway cloning (Invitrogen, USA). In the first round the DmGucy2d coding sequence was amplified using primers located on each of the untranslated regions. For the second PCR, 2 µl of unpurified PCR product of the first PCR was used as a template. Primers containing appropriate sequences for gateway cloning were used for the second PCR. The coding sequence was cloned without the stop codon to allow for gene fusion at the C-terminus. Tagging at the N-terminus was not considered, since the protein is predicted to undergo cleavage of the signal peptide (30 amino acids, Supplemental Figure 4B, arrowhead). The coding sequence was confirmed through sequencing and sub-cloned into pTWG (Drosophila Genomic Resource Centre) for C-terminal fusion with GFP.

Plasmid DNA was amplified in *E. coli* DH5α and purified using ZR Plasmid Miniprep™-Classic (Zymo research, USA). ZymoPURE™ Midiprep Kit (Zymo

research, USA) was used for large scale DNA purification that is required (*Dmift88*, *DmGucy2d* or T1-*DmGucy2d* in pTWG) for transfection experiments and fly transgenesis. Injections into *Drosophila* embryos and selection of positive transformants were outsourced (BestGene, USA or IGC transgenics facility, Portugal).

Detection of *DmGucy2d* gene expression: In order to detect expression of *DmGucy2d* in different developmental stages, an enhancer Gal4-trap line (CG34357[NP0270]) was obtained (Brand and Perrimon, 1993). Flies carrying the enhancer trap insertion were crossed with flies encoding 40xUAS-IVS-mCD8::GFP. The mCD8::GFP fusion protein is targeted to the membrane of the cells and was used to visualize the morphology of cells. 40 UAS tandem insertions were chosen to increase the signal intensity.

For imaging adult antenna, the cuticle of the heads was cleared as further explained below, and the second antenna segment was imaged entirely on an SP5 Live Upright microscope (Leica, Germany). Confocal Z-stack images were deconvolved using the Huygens v17.4 software (SVI, Netherlands) and 3D reconstructed using the Imaris v6.4 software (Bitplane, USA), which was also used to prepare the movie (Supplemental movie 02). Wandering L3 larvae were mounted and imaged as described for the live-imaging of L3 larvae below.

Live imaging of chordotonal cilia in L3 larvae

GFP::*Dmift88* was expressed in chordotonal neurons using Gal4^{lav} (Gong et al., 2004b). Flies were reared at 25°C to the third larval stage and all experiments were performed with wandering L3 larvae. Larvae were collected and briefly washed in PBS. For imaging, larvae were immobilised between a coverslip and a slide in a drop of PBS (Zhang et al., 2013). The cover slip was held in place using transparent double-sticky tape. Imaging was performed using a Roper Spinning Disc microscope (Nikon). Samples were kept at 25°C through the imaging process. To prevent artefacts from cell death, larvae were always imaged immediately after immobilisation and for a maximum duration of two minutes. Images were acquired every 120 ms with 100 ms exposure time. Images were analysed using the FIJI software (Schindelin et al., 2012) and kymographs were generated using the KymographClear plugin (Mangeol et al., 2016). Data plots were generated using RStudio (RStudio®, USA).

Quantification of *DmIFT88* expression levels from adult antennae

For measuring *Dmift88* expression levels, the total mRNA was isolated from antennae of adult flies with specific genotypes up to four days after eclosure using Real-time PCR (RT-PCR). The web browser-based Primer-BLAST tool (Ye et al., 2012) was used to design primers specific for a given transcript. At least one primer in a pair was designed to span an exon-exon junction in order to avoid amplification of genomic DNA that might contaminate the samples. All primers (see Supplemental Table 06) used in this study were tested to only yield a single product and to not amplify genomic DNA. The *Dmift88* primers were confirmed to only amplify the respective isoform using cDNA (data not shown). 150 ng of total mRNA were reverse transcribed to cDNA in a reaction volume of 20 μ l. The cDNA mix was diluted 1:10, and 4 μ l of the dilutions were used in each reaction. iTaq™ Universal SYBR® Green Supermix (Biorad USA) was used to detect amplification of the PCR products. The reactions were set-up up according to the manufacturers protocol and run on the CFX384 Touch™ Real-Time PCR Detection System (Biorad, USA). The total mRNA was isolated three times per genotype and each sample was measured in triplicates. Results were analysed using RStudio (Rstudio®, USA).

Sound evoked neuronal responses

Recordings of sound-evoked compound action potentials of chordotonal neurons in the fly's 2nd antennal segment were performed as previously reported (Bechstedt et al., 2010). Measurements were carried out using flies up to six days after eclosure. Action potentials were recorded from head-fixed flies. For recording, a tungsten needle was inserted between head and antenna. The other antenna was immobilised, and the reference electrode was positioned in the thorax. To determine maximum compound action potential amplitudes, flies were stimulated with pure tones at the individual best frequency of their antenna, which was determined from the velocity spectrum of the antenna's mechanical free fluctuations measured with a scanning laser Doppler vibrometer (PSV-400, Polytec, Waldbronn, Germany) (for details, see (Gopfert et al., 2005)). Data was analysed and graphs were generated using RStudio (RStudio®, USA).

Sample preparation and image acquisition in Transmission Electron Microscope

The samples for electron microscopy were processed and sectioned as previously described (Jana *et al.*, 2016). Antennae were dissected from the heads and incubated in fixative (2% formaldehyde, 2.5% glutaraldehyde in 0.1 M sodium biphosphate buffer pH 7.2–7.4) overnight. Samples were washed several times in PBS and then incubated for 1.5 hours in 1% osmium tetroxide for postfixation. Samples were washed several times in deionised water before incubating them in 2% uranyl acetate for 20 minutes on a rotator for *en bloc* staining. After this step, samples were dehydrated in a graded sequence of alcohol dilutions (from 50% to a 100%). Ethanol was removed through two incubation steps with propylene oxide for 30 min. Samples were embedded in resin overnight and transferred to a fresh batch of resin for 1h. Under a dissection microscope, the second segment of the antenna was separated from the third. The second segment was placed in the desired orientation into a mold with resin and polymerised. Samples were sectioned ~70 nm thick, collected on formvar-coated copper slot grids and stained with 2% uranyl acetate followed by lead citrate staining. Finally, samples were air-dried and investigated and photographed at 100kV using the Hitachi H-7650 transmission electron microscope.

Conditional knockdown in the flies

The Gal4^{Chat19b} driver is active in cholinergic neurons, including chordotonal and olfactory neurons, in all developmental stages of the fly (Jana *et al.*, 2011; Salvaterra and Kitamoto, 2001). Thus, to avoid confounding effects from the ciliogenesis defects and be able to spatiotemporally knockdown our gene of interest in the adults, we adopted a Gal4^{Chat19b}-*TubGal80^{ts}*-UAS-RNAi-based system. The Gal4 activity was repressed through co-expression of a temperature sensitive version of Gal80 under *Tubulin* promoter (denoted as *TubGal80^{ts}*) (McGuire *et al.*, 2003). At the permissive temperature (18°C) *TubGal80^{ts}* is functional, acting as a negative regulator by binding to Gal4 and preventing it from attracting polymerase to a UAS element in the fly genome (del Valle Rodriguez *et al.*, 2011). Thus, a candidate (i.e. *Dmift88*, *DmGucy2d*) mRNA will only be reduced through RNAi if flies are kept at the restrictive temperature (29°C). Flies were reared at 18°C, shifted to the restrictive temperature after eclosure (when ciliogenesis is finished), and then submitted to the climbing (negative-gravitaxis) assay for up to two weeks (also see, Figure 2A).

Climbing (or negative-gravitaxis) assay

To quantify climbing behaviour, a behavioural readout of sensory function, flies were collected in 24-hour time windows and kept in groups of the same age. The animals were transferred to vials with fresh food every three days. Prior to the behaviour experiments, flies were separated according to sex into groups of ten animals that would be tested jointly. Flies were briefly anaesthetised using CO₂ for sorting. The flies were kept in the room where the behavioural experiments were conducted for about one hour prior to the actual experiment. This time period was given to allow the animals to acclimatise to potentially different light and temperature regimes. Experiments were conducted in measuring cylinders made of glass. Animals were placed in cylinders a couple of minutes before the assay was started. Cylinders were sealed on top with perforated parafilm to prevent the flies from escaping. Cylinders were tapped until all flies were at the bottom of the cylinder and flies were subsequently allowed to walk up. All experiments were videotaped for one minute and analysed blindly only once a full data set (including control flies) was obtained. The metric used for analysis was the number of flies above ten centimetres after ten seconds, as, in the set-up. The flies expressing a hairpin against *mCherry* (UAS-*mCherry*-IR; negative control) in cholinergic neurons need on average ten seconds to perform this task. Videos were analysed for the whole duration of ten seconds after tapping the cylinder, to rule out that flies reached the ten-centimetre mark and walked back down again. Data was analysed and graphs were generated using RStudio (RStudio®, USA).

Cell culture and immunoprecipitation experiments

For co-immunoprecipitation of ectopically expressed proteins, *Drosophila melanogaster* (Dmel) cultured cells were co-transfected with the corresponding constructs (GFP tagged at the C-terminus of either DmGucy2d full-length or fragments (T1-T5)) with 3xHA::DmIFT88. The co-overexpression of GFP alone with 3xHA::DmIFT88 serves as a negative control in these experiments. Cells were seeded at a density of 3x10⁶ cells/well in 6-well plates (Orange Scientific). One hour later they were transfected using Effectene Transfection Reagent (Quiagen) according to manufacturer (see Supplementary Table 06 for primers information). Cells were harvested three days after transfection. Cells were resuspended, the suspension was collected and centrifuged and pellets were stored at -80°C, if not processed immediately. Ectopically expressed DmGucy2d::GFP was immunoprecipitated at 4°C

for 2 hrs from Dmel cell lysates (three wells in total for each condition per experiment) using polyclonal anti-GFP antibodies and protein A or G magnetic Dynabeads (Thermo Fisher Scientific). 2 µg anti-GFP antibodies were added to protein-A or -G magnetic beads and incubated for 30 min at room temperature. Cells were homogenised in lysis buffer: 50 mM Tris-HCl pH 8, 250 mM NaCl, 1 mM DTT, 2% NP-40, 0.5% of SDS, 0.5% sodiumdeoxycholate, 1× protease inhibitor, 5µg/ml Leupeptin and 15µg/ml Aprotinin, 0.1% Digitonin at 4 C for 30 min. Then, benzonase was added to the lysate (final concentration 0.25 units/µl) and incubated for another 15 min. After centrifugation at 13,500 g for 20 min at 4°C, the pre-cleared supernatants were incubated with the coupled beads with antibodies. After several washes with lysis buffer, bead pellets were boiled in SDS sample buffer, separated by 4-15 % gradient SDS-PAGE and transferred onto LI-COR nitrocellulose membranes for Odyssey. GFP, DmGucy2d::GFP constructs and HA::DmIFT88 were visualised with anti-GFP or anti-HA antibodies. Secondary LI-COR antibodies IRDye 680RD over IRDye 800 (LI-COR) were used as a second step (see Supplementary Table 05 for details on the antibodies used).

Cuticle clearing and imaging of antennae whole-mounts

The cuticle of the adult flies is opaque and autofluorescent, which makes this organ generally unsuitable for imaging. A clearing method that made the cuticle transparent without affecting the morphology of the cells/tissues was developed to image the cytoplasmic GFP expressed in the chordotonal neurons in the adult flies with different genotypes. It allowed imaging of the whole antenna without mechanical manipulation. The whole heads were fixed in 4 % of paraformaldehyde in PBS (supplemented with 0.05 % Triton-X) for 40 minutes on ice (Kolesova et al., 2016). Heads were then transferred to a reaction tube containing FocusClear (CelExplorer, Taiwan) and incubated overnight. For imaging, heads were mounted on a slide in MountClear (CelExplorer, Taiwan). Several layers of clear tape were used as spacer between slide and coverslip. Images were acquired on a SP5 Upright microscope (Leica, Germany). The size of the image stack was chosen to contain the whole antenna segment. Images were then analysed using ImageJ or Imaris v6.4 software (Bitplane).

Statistical analysis

All statistical analyses were performed using either RStudio (RStudio®, USA) or Prism (GraphPad Software, USA). The details of the statistical methods used to analyse a given set of experiments are mentioned in the relevant figure legends.

References:

- Bechstedt, S., J.T. Albert, D.P. Kreil, T. Muller-Reichert, M.C. Gopfert, and J. Howard. 2010. A doublecortin containing microtubule-associated protein is implicated in mechanotransduction in *Drosophila* sensory cilia. *Nature communications*. 1:11.
- Besschetnova, T.Y., E. Kolpakova-Hart, Y. Guan, J. Zhou, B.R. Olsen, and J.V. Shah. 2010. Identification of signaling pathways regulating primary cilium length and flow-mediated adaptation. *Current biology : CB*. 20:182-187.
- Cheng, L.E., W. Song, L.L. Looger, L.Y. Jan, and Y.N. Jan. 2010. The role of the TRP channel NompC in *Drosophila* larval and adult locomotion. *Neuron*. 67:373-380.
- de Castro-Miro, M., E. Pomares, L. Lores-Motta, R. Tonda, J. Dopazo, G. Marfany, and R. Gonzalez-Duarte. 2014. Combined genetic and high-throughput strategies for molecular diagnosis of inherited retinal dystrophies. *PloS one*. 9:e88410.
- del Valle Rodriguez, A., D. Didiano, and C. Desplan. 2011. Power tools for gene expression and clonal analysis in *Drosophila*. *Nature methods*. 9:47-55.
- Edgar, R.C. 2004. MUSCLE: multiple sequence alignment with high accuracy and high throughput. *Nucleic acids research*. 32:1792-1797.
- Feng, X., T. Wei, J. Sun, Y. Luo, Y. Huo, P. Yu, J. Chen, X. Wei, M. Qi, and Y. Ye. 2020. The pathogenicity of novel GUCY2D mutations in Leber congenital amaurosis 1 assessed by HPLC-MS/MS. *PloS one*. 15:e0231115.
- Fu, J., and D.M. Glover. 2012. Structured illumination of the interface between centriole and peri-centriolar material. *Open biology*. 2:120104.
- Gong, Z., W. Son, Y.D. Chung, J. Kim, D.W. Shin, C.A. McClung, Y. Lee, H.W. Lee, D.J. Chang, B.K. Kaang, H. Cho, U. Oh, J. Hirsh, M.J. Kernan, and C. Kim. 2004. Two interdependent TRPV channel subunits, inactive and Nanchung, mediate hearing in *Drosophila*. *The Journal of neuroscience : the official journal of the Society for Neuroscience*. 24:9059-9066.
- Gopfert, M.C., A.D. Humphris, J.T. Albert, D. Robert, and O. Hendrich. 2005. Power gain exhibited by motile mechanosensory neurons in *Drosophila* ears. *Proceedings of the National Academy of Sciences of the United States of America*. 102:325-330.
- Han, Y.G., B.H. Kwok, and M.J. Kernan. 2003. Intraflagellar transport is required in *Drosophila* to differentiate sensory cilia but not sperm. *Current biology : CB*. 13:1679-1686.
- He, M., R. Subramanian, F. Bangs, T. Omelchenko, K.F. Liem, Jr., T.M. Kapoor, and K.V. Anderson. 2014. The kinesin-4 protein Kif7 regulates mammalian Hedgehog signalling by organizing the cilium tip compartment. *Nature cell biology*. 16:663-672.
- Ishikawa, H., T. Ide, T. Yagi, X. Jiang, M. Hirono, H. Sasaki, H. Yanagisawa, K.A. Wemmer, D.Y. Stainier, H. Qin, R. Kamiya, and W.F. Marshall. 2014.

- TTC26/DYF13 is an intraflagellar transport protein required for transport of motility-related proteins into flagella. *eLife*. 3:e01566.
- Jacobson, S.G., A.V. Cideciyan, I.V. Peshenko, A. Sumaroka, E.V. Olshevskaya, L. Cao, S.B. Schwartz, A.J. Roman, M.B. Olivares, S. Sadigh, K.W. Yau, E. Heon, E.M. Stone, and A.M. Dizhoor. 2013. Determining consequences of retinal membrane guanylyl cyclase (RetGC1) deficiency in human Leber congenital amaurosis en route to therapy: residual cone-photoreceptor vision correlates with biochemical properties of the mutants. *Human molecular genetics*. 22:168-183.
- Jana, S.C., M. Girotra, and K. Ray. 2011. Heterotrimeric kinesin-II is necessary and sufficient to promote different stepwise assembly of morphologically distinct bipartite cilia in *Drosophila* antenna. *Molecular biology of the cell*. 22:769-781.
- Jana, S.C., S. Mendonca, S. Werner, and M. Bettencourt-Dias. 2016. Methods to Study Centrosomes and Cilia in *Drosophila*. *Methods in molecular biology*. 1454:215-236.
- Karpenahalli, M.R., A.N. Lupas, and J. Soding. 2007. TPRpred: a tool for prediction of TPR-, PPR- and SEL1-like repeats from protein sequences. *BMC bioinformatics*. 8:2.
- Kolesova, H., M. Capek, B. Radochova, J. Janacek, and D. Sedmera. 2016. Comparison of different tissue clearing methods and 3D imaging techniques for visualization of GFP-expressing mouse embryos and embryonic hearts. *Histochemistry and cell biology*. 146:141-152.
- Kuhn, M. 2016. Molecular Physiology of Membrane Guanylyl Cyclase Receptors. *Physiological reviews*. 96:751-804.
- Lee, N., J. Park, Y.C. Bae, J.H. Lee, C.H. Kim, and S.J. Moon. 2018. Time-Lapse Live-Cell Imaging Reveals Dual Function of Oseg4, *Drosophila* WDR35, in Ciliary Protein Trafficking. *Molecules and cells*. 41:676-683.
- Li, A., M. Saito, J.Z. Chuang, Y.Y. Tseng, C. Dedesma, K. Tomizawa, T. Kaitsuka, and C.H. Sung. 2011. Ciliary transition zone activation of phosphorylated Tctex-1 controls ciliary resorption, S-phase entry and fate of neural progenitors. *Nature cell biology*. 13:402-411.
- Liu, X., K. Fujinami, K. Kuniyoshi, M. Kondo, S. Ueno, T. Hayashi, K. Mochizuki, S. Kameya, L. Yang, Y. Fujinami-Yokokawa, G. Arno, N. Pontikos, H. Sakuramoto, T. Kominami, H. Terasaki, S. Katagiri, K. Mizobuchi, N. Nakamura, K. Yoshitake, Y. Miyake, S. Li, T. Kurihara, K. Tsubota, T. Iwata, K. Tsunoda, and C. Japan Eye Genetics. 2020. Clinical and Genetic Characteristics of 15 Affected Patients From 12 Japanese Families with GUCY2D-Associated Retinal Disorder. *Translational vision science & technology*. 9:2.
- Mangeol, P., B. Prevo, and E.J. Peterman. 2016. KymographClear and KymographDirect: two tools for the automated quantitative analysis of molecular and cellular dynamics using kymographs. *Molecular biology of the cell*. 27:1948-1957.
- McGuire, S.E., P.T. Le, A.J. Osborn, K. Matsumoto, and R.L. Davis. 2003. Spatiotemporal rescue of memory dysfunction in *Drosophila*. *Science*. 302:1765-1768.
- Morton, D.B. 2004. Atypical soluble guanylyl cyclases in *Drosophila* can function as molecular oxygen sensors. *The Journal of biological chemistry*. 279:50651-50653.

- Mourao, A., S.T. Christensen, and E. Lorentzen. 2016. The intraflagellar transport machinery in ciliary signaling. *Current opinion in structural biology*. 41:98-108.
- Nielsen, H. 2017. Predicting Secretory Proteins with SignalP. *Methods in molecular biology*. 1611:59-73.
- Roca, A.I., A.E. Almada, and A.C. Abajian. 2008. ProfileGrids as a new visual representation of large multiple sequence alignments: a case study of the RecA protein family. *BMC bioinformatics*. 9:554.
- Salehi Chaleshtori, A.R., M. Garshasbi, A. Salehi, and M. Noruzinia. 2020. The Identification and Stereochemistry Analysis of a Novel Mutation p.(D367Tfs*61) in the CYP1B1 Gene: A Case Report. *Journal of current ophthalmology*. 32:114-118.
- Salvaterra, P.M., and T. Kitamoto. 2001. Drosophila cholinergic neurons and processes visualized with Gal4/UAS-GFP. *Brain research. Gene expression patterns*. 1:73-82.
- Schindelin, J., I. Arganda-Carreras, E. Frise, V. Kaynig, M. Longair, T. Pietzsch, S. Preibisch, C. Rueden, S. Saalfeld, B. Schmid, J.Y. Tinevez, D.J. White, V. Hartenstein, K. Eliceiri, P. Tomancak, and A. Cardona. 2012. Fiji: an open-source platform for biological-image analysis. *Nature methods*. 9:676-682.
- Tran, P.V., C.J. Haycraft, T.Y. Besschetnova, A. Turbe-Doan, R.W. Stottmann, B.J. Herron, A.L. Chesebro, H. Qiu, P.J. Scherz, J.V. Shah, B.K. Yoder, and D.R. Beier. 2008. THM1 negatively modulates mouse sonic hedgehog signal transduction and affects retrograde intraflagellar transport in cilia. *Nature genetics*. 40:403-410.
- Tucker, C.L., V. Ramamurthy, A.L. Pina, M. Loyer, S. Dharmaraj, Y. Li, I.H. Maumenee, J.B. Hurley, and R.K. Koeneke. 2004. Functional analyses of mutant recessive GUCY2D alleles identified in Leber congenital amaurosis patients: protein domain comparisons and dominant negative effects. *Molecular vision*. 10:297-303.
- Wei, Q., Y. Zhang, Y. Li, Q. Zhang, K. Ling, and J. Hu. 2012. The BBSome controls IFT assembly and turnaround in cilia. *Nature cell biology*. 14:950-957.
- Williams, C.L., J.C. McIntyre, S.R. Norris, P.M. Jenkins, L. Zhang, Q. Pei, K. Verhey, and J.R. Martens. 2014. Direct evidence for BBSome-associated intraflagellar transport reveals distinct properties of native mammalian cilia. *Nature communications*. 5:5813.
- Wolff, A., B. de Nechaud, D. Chillet, H. Mazarguil, E. Desbruyeres, S. Audebert, B. Edde, F. Gros, and P. Denoulet. 1992. Distribution of glutamylated alpha and beta-tubulin in mouse tissues using a specific monoclonal antibody, GT335. *European journal of cell biology*. 59:425-432.
- Yates, A., W. Akanni, M.R. Amode, D. Barrell, K. Billis, D. Carvalho-Silva, C. Cummins, P. Clapham, S. Fitzgerald, L. Gil, C.G. Giron, L. Gordon, T. Hourlier, S.E. Hunt, S.H. Janacek, N. Johnson, T. Juettemann, S. Keenan, I. Lavidas, F.J. Martin, T. Maurel, W. McLaren, D.N. Murphy, R. Nag, M. Nuhn, A. Parker, M. Patricio, M. Pignatelli, M. Rahtz, H.S. Riat, D. Sheppard, K. Taylor, A. Thormann, A. Vullo, S.P. Wilder, A. Zadissa, E. Birney, J. Harrow, M. Muffato, E. Perry, M. Ruffier, G. Spudich, S.J. Trevanion, F. Cunningham, B.L. Aken, D.R. Zerbino, and P. Flicek. 2016. Ensembl 2016. *Nucleic acids research*. 44:D710-716.
- Ye, F., D.K. Breslow, E.F. Koslover, A.J. Spakowitz, W.J. Nelson, and M.V. Nachury. 2013. Single molecule imaging reveals a major role for diffusion in the exploration of ciliary space by signaling receptors. *eLife*. 2:e00654.

- Ye, J., G. Coulouris, I. Zaretskaya, I. Cutcutache, S. Rozen, and T.L. Madden. 2012. Primer-BLAST: a tool to design target-specific primers for polymerase chain reaction. *BMC bioinformatics*. 13:134.
- Zagel, P., and K.W. Koch. 2014. Dysfunction of outer segment guanylate cyclase caused by retinal disease related mutations. *Frontiers in molecular neuroscience*. 7:4.